Protein Secondary Structure Controlled with Light and Photoresponsive Surfactants

Shao-Chun Wang and C. Ted Lee, Jr.*

Department of Chemical Engineering and Material Science, University of Southern California, Los Angeles, California 90089-1211

Received: February 15, 2006; In Final Form: May 31, 2006

The interaction of a light-responsive azobenzene surfactant with bovine serum albumin (BSA) has been investigated as a means to examine photoreversible changes in protein secondary structure. The cationic azobenzene surfactant undergoes a reversible photoisomeriztion upon exposure to the appropriate wavelength of light, with the visible-light (trans) form being more hydrophobic and, thus, inducing a greater degree of protein unfolding than the UV-light (cis) form. Fourier transform infrared (FT-IR) spectroscopy is used to provide quantitative information on the secondary structure elements in the protein (α-helices, β-strands, β-turns, and unordered domains). Comparing the secondary structure changes induced by light illumination in the presence of the photoresponsive surfactant with previous measurements of the tertiary structure of BSA obtained from small-angle neutron scattering (SANS) allows the three discrete conformation changes in BSA to be fully characterized. At low surfactant concentrations, an α-helix → β-structure rearrangement is observed as the tertiary structure of BSA changes from a heart-shaped to a distorted heart-shaped conformation. Intermediate surfactant concentrations lead to a dramatic decrease in the α-helix fraction in favor of unordered structures, which is accompanied by an unfolding of the C-terminal portion of the protein as evidenced from SANS. Further increases in photosurfactant concentration lead to a β → unordered transition with the protein adopting a highly elongated conformation in solution. Each of these protein conformational changes can be precisely and reversibly controlled with light illumination, as revealed through FT-IR spectra collected during repeated visible-light ↔ UV-light cycles.

Introduction

Proteins are polyelectrolyte chains formed from a specific sequence of the 20 naturally occurring amino acids, termed the *primary structure* of the protein. As a result of differing degrees of water affinity of these amino acids, the protein folds such that the free energy is minimized, preferentially with hydrophobic amino acids in the core and hydrophilic amino acids on the surface of the protein. This folding is manifested locally by the formation of *secondary structure* elements such as α-helices and β-sheets that are stable due to simultaneously minimizing the strain on the relatively rigid amide linkages, while at the same time maximizing the formation of hydrogen bonds. Ultimately, these elements arrange into the overall shape or *tertiary structure* of the protein. These folding events, which lead to the formation of the native state, give rise to a functional protein. However, proteins are not static entities and instead regularly undergo conformational changes to intermediately folded states during the course of activity, particularly upon interaction with ligands or substrates. As such, precise knowledge of how a protein unfolds/refolds in response to various stimuli is required for complete understanding of the form−function relationship of a protein.

To achieve this goal, photoresponsive surfactants can be utilized as a means of reversibly controlling protein conformation with simple light illumination.[1,2] Since protein folding results from interactions between the protein amino acids and the solvent (i.e., hydrophobic, electrostatic, van der Waals, and hydrogen bonding), altering these intramolecular forces responsible for maintaining the secondary and tertiary structures results in changes in protein conformation.[3,4] Indeed, on the basis of the importance of protein folding in biological, chemical, and industrial applications, extensive efforts have been devoted to probe conformational changes in proteins with pH, temperature, pressure, and chemical denaturants. Among these denaturants, surfactants (i.e., molecules containing both a hydrophobic tail and a hydrophilic, typically charged headgroup) can provide specific insight into protein folding processes, particularly when considering that proteins routinely come in contact with a variety of amphiphilic molecules (e.g., cell membranes, surfactant-assisted solubilization and crystallization, etc.). Surfactants bound to a protein generally shield the unfavorable interaction of the nonpolar amino acids of the protein with water, allowing the protein to unfold.[5,6]

In the case of azobenzene-based photoresponsive surfactants, which as shown in Figure 1 undergo a reversible trans ↔ cis photoisomerization upon exposure to visible and UV light, respectively,[7−11] enhanced protein−surfactant interactions occur under visible light as a consequence of the relative hydrophobicity of the planar trans isomer compared to the bent cis conformation, leading to protein unfolding that can be reversed with exposure to UV light.[1,2] Direct photocontrol of the folding of bovine serum albumin (BSA) was demonstrated with *in vitro* tertiary structures obtained by applying shape-reconstruction techniques to small-angle neutron scattering (SANS) data. Three discrete folding forms of BSA were detected, including a heart-shaped *N* form at low surfactant concentrations (similar to the native-state X-ray crystallographic structure[12]), a partially unfolded *F* form at intermediate surfactant concentrations (with the C-terminal portion separated from the remainder of the protein), and a highly elongated *E* form at high surfactant

* Corresponding author. Office: 213-740-2066. E-mail: tedlee@usc.edu.

10.1021/jp060981n CCC: $33.50
Published on Web 07/25/2006

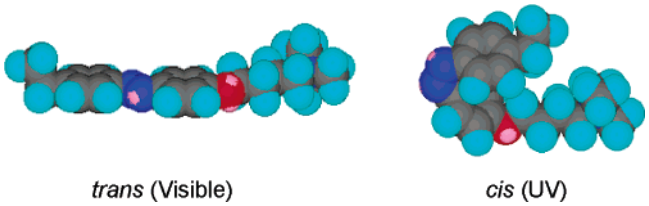

Figure 1. Space-filling model of the azobenzene-based photoresponsive surfactants. Left: trans isomer under visible-light (436-nm) illumination; right: cis isomer under UV-light (365-nm) illumination.

concentrations (although some residual folding, i.e., "kinks", were evident in the shape-reconstructed conformations), while $N \leftrightarrow F$ and $F \leftrightarrow E$ transitions could be induced with light. The structure of BSA is dominated by nine helical loops connected with 17 disulfide bridges (the three protein domains each contain one small and two large helical loops), leading to a secondary structure of approximately 67% helical content with the remainder consisting of ~23% extended conformations (β-strands) and ~10% β-turns.[13−15] Upon unfolding under acid conditions[16] or through the addition of surfactants,[17,18] the helicity of BSA decreases but still represents ~50% of the secondary structure, suggesting that the six large helical loops in BSA are not disrupted.[19]

In the present study, we utilize measurements of the secondary structure of BSA in response to photoresponsive surfactant and light illumination as a means of investigating the local reversibility of photocontrolled protein folding. By using Fourier transform infrared (FT-IR) spectroscopy, quantitative information on the changes in the BSA secondary structure induced by photosurfactant and light illumination are obtained. Comparing changes in secondary (FT-IR) and tertiary (SANS) structures observed during the $N \rightarrow F$ and $F \rightarrow E$ transitions, while at the same time reversibly controlling these transitions with light, provides unique insight into the mechanisms of BSA folding.

Experimental Details

An azobenzene trimethylammonium bromide surfactant (azoTAB) of the form

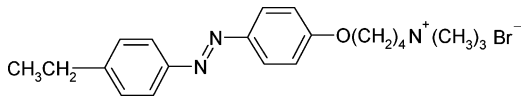

was synthesized according to published procedures.[7,20] Conversion from the trans form to the cis isomer was achieved by illumination with a 200-W mercury arc lamp (Oriel, model no. 6283) equipped with a 320-nm band-pass filter (Oriel, model no. 59800) in combination with a heat-absorbing IR filter (Oriel, model no. 59060) to isolate the 365-nm line. For conversion from the cis form to the trans form, a 400-nm long-pass filter (Oriel, model no. 59472) was used to illuminate the sample with the 436-nm line from the mercury lamp. Absorption measurements indicate that under visible light the surfactant exhibits an approximately 75/25 trans/cis equilibrium, while under UV light the surfactant is primarily in the cis form (>90% cis).[21]

Highest-quality BSA was purchased from Roche and used as received. Samples were prepared by dissolving 10 mg/mL BSA and varying amounts of crystallized surfactant into a D_2O phosphate buffer solution (8.3 mM, pD = 7.30 measured with a standard pH electrode and corrected according to pD = pH + 0.4 for deuterium isotope effects). Samples were prepared 48 h prior to FT-IR measurements to ensure complete H−D exchange.

Infrared spectra were measured with a Genesis II FT-IR spectrometer (Mattson Instruments). Solutions were loaded between a pair of CaF_2 windows using a 50-μm Teflon spacer contained in a demountable liquid cell equipped with a circulating water jacket (T = 20 °C). A liquid light guide (Oriel, model no. 77557) was oriented within the spectrometer to directly illuminate the sample with UV or visible light for 90 min prior to and during data collection. The sample chamber was continuously purged with dry air to eliminate water vapor. For each spectrum, a 250-scan interferogram was collected with a 4-cm^{-1} resolution. The absorbance due only to the protein secondary structure was obtained by subtracting the spectra measured for a pure surfactant solution under otherwise identical conditions, allowing the relatively sharp surfactant peaks at ~1600 cm^{-1} to be removed. The resulting corrected spectra were flat in the region between 2000 and 1750 cm^{-1} and were used for further analysis. The technique of Fourier self-deconvolution (FSD) was applied to the original spectra to resolve the overlapping bands in the amide I region using a band-narrowing factor k = 2.0 and a full width at half-height of 25.15 cm^{-1}. Second-derivative spectra were obtained with the Savitsky-Golay function for a third-order polynomial, using a five-data-point window. Difference spectra at varying surfactant concentration were obtained by subtracting the spectra collecting under visible-light from the spectra collecting under UV-light illumination. For pure BSA solutions, the difference spectra showed no significant absorbance (<1% throughout the amide I region). Curve-fitting was carried out on the deconvolved spectra by assuming Gaussian band profiles. The number of peaks and initial values for the peak positions, intensities, widths, and heights were estimated from the second derivative and deconvolved spectra. The percentages of each structural component were estimated from the relative areas of each curve.

Results and Discussion

FT-IR Spectra of BSA−azoTAB Mixtures. Figure 2, parts a−d, shows the FSD and second derivative spectra of BSA solutions in the amide I region of 1700−1600 cm^{-1} with varying azoTAB surfactant concentration under visible (trans form) and UV (cis form) light. In the absence of surfactant, the spectrum for pure BSA can be resolved into four major bands as shown in Figure 2a, which can be assigned according to the literature[22−27] as 1677 cm^{-1} (β-turns), 1653 cm^{-1} (α-helices), 1630 cm^{-1} (β-strands, short segments connecting helical structures), and 1610 cm^{-1} (vibrations of the aromatic side chains). In addition, a minor peak (~2% of the total structure) is found at approximately 1641 cm^{-1}, which will be discussed below.

As the surfactant concentration is increased under either visible or UV light, a broad band develops in the region of ~1645 cm^{-1} (particularly evident under visible light, see Figure 2, parts a and c), which is a typical location for unordered structures. At the same time, the influence of the α-helix peak on the spectra decreases, resulting in the maximum in the amide I band shifting to lower wavenumbers and indicating a loss of secondary structure (primarily a helix-to-unordered transition) as BSA unfolds. The second derivative spectra (Figure 2, parts c and d) also indicate a gradual decreases in the α-helical band accompanied by an increase in unordered structures with increasing surfactant concentration. While similar trends are seen under both visible and UV light, the effects are less obvious and require higher surfactant concentrations with UV illumination, as the more hydrophobic trans form of the surfactant results in a greater degree of protein unfolding compared to the cis isomer. As discussed below, the appearance of the unordered

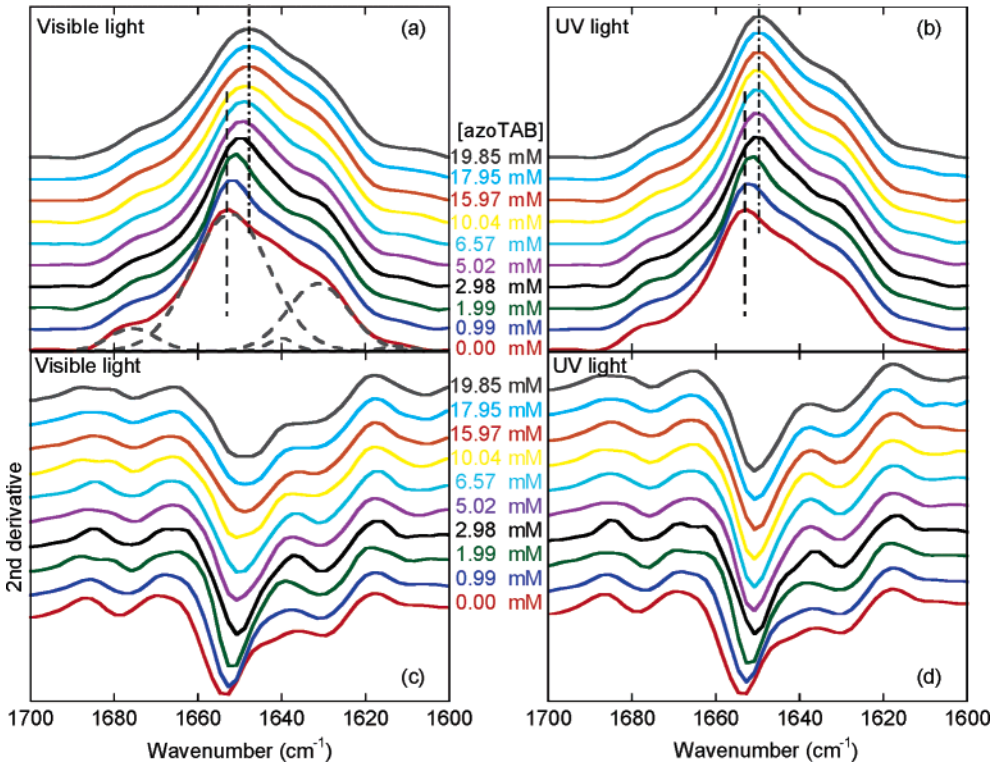

Figure 2. Deconvolved FT-IR spectra of BSA in solution with varying azoTAB surfactant concentration under (a) visible and (b) UV light, respectively. The maximum of the amide I band is shifting to lower wavenumber with increasing surfactant concentration. Vertical dashed lines in (a) and (b) indicate the maximum of the amide I band without surfactant (---) and with 19.85 mM azoTAB surfactant (−·−), respectively. Dashed curves in (a) show the individual Gaussian band for each secondary structure element of pure BSA (see text). Also shown are the second derivatives of the FT-IR spectra under (c) visible, and (d) UV light, respectively.

peak in Figure 2 coincides with the discrete unfolding of BSA to the *F* form observed with SANS,[1] while the continual shift in the peak maximum is consistent with the $F \rightarrow E$ transition observed at higher surfactant concentrations.

The minor peak found in the spectrum for pure BSA at 1641 cm^{-1} is difficult to unequivocally define. Although this region is typically assigned to random or unordered structures, as was done above for the broad peak that develops at 1645 cm^{-1}, comparing the X-ray crystallographic structure of serum albumin to various spectroscopic techniques and sequence-based predictive methods generally indicates that native BSA contains no unordered domains.[13,14] A "hydrated peak" at ∼1640 cm^{-1} has also been attributed to either β-turn or random conformations within the protein core that contain bound water molecules,[28,29] perhaps forming hydrogen bonds within the loops of the β-turns and thereby disrupting the turn structure,[30] consistent with the idea that BSA, even in the crystalline state, is known to contain a large amount of bound water.[13,14] As seen from the second derivative spectra in Figure 2, parts c and d, the 1641 cm^{-1} peak is evident only at low surfactant concentrations (below 1 mM and 3 mM azoTAB under visible and UV light, respectively, while at 2 mM azoTAB this peak could be reversibly disrupted and reformed with cycles of visible- and UV-light exposure), supporting the assignment to a hydrated peak with surfactant binding potentially replacing bound water molecules. Indeed, the core of BSA becomes accessible to the hydrophobic probe Nile red at an azoTAB concentration of ∼1 mM under visible light, while at the same time the heart-shaped structure of BSA becomes somewhat distorted.[1] Despite this evidence, it is beyond the resolution of FT-IR to definitively assign the origin of this peak, thus, the simplified approach of assigning all peaks in the region of 1645−1640 cm^{-1} to unordered structures is utilized.

Quantitative Analysis of the FT-IR Spectra. To determine the individual contributions to the overall protein secondary structure, the FSD spectra were deconvoluted into five peaks (β-turns at 1677 cm^{-1}, α-helices at 1653 cm^{-1}, unordered structures at 1640 cm^{-1}, β-strands at 1630 cm^{-1}, and side-chain vibrations at 1610 cm^{-1}) as shown in Figure 3. The results for pure BSA indicate 65% α-helix, 25% β-strand, 6% β-turn, and 2% unordered structures, with ∼1% of the structure occurring in the side-chain region. The α-helix percentage has generally been reported to range from 55 to 60% using FT-IR[24,31−33] or Raman[34] spectroscopy and up to 68% using CD[17,35] spectroscopy, while a value of 65% has been estimated from the sequences of several albumins.[36] Values in the literature for the percentage of β-structures vary more widely, however, ranging from 35 to 44% using FT-IR (22−30% β-strand and 11−16% β-turn)[24,31−33] and from 3 to 30% with CD (β-strand), while X-ray crystallography indicates that ∼33% of the protein exists as β-structures.[37]

As shown in Figure 3, each secondary structure component changes in a nonmonotonic manner in response to surfactant concentration and light illumination. The α-helix percentage (Figure 3a) decreases to an intermediate plateau value at low surfactant concentrations, followed by a second depression and eventually reaching a constant value of ∼50%. In addition, less α-helical character is consistently observed when illuminating with visible compared to UV light. At the same time, the percentage of unordered structures (Figure 3c) is seen to increase with increasing surfactant concentration, with a greater unordered component found under visible light. The β-turn and β-strand structures in Figure 3, parts b and d, respectively, initially increase with surfactant addition and then gradually decrease at higher surfactant concentrations (especially the β-strand content), with the loss of β-structure again occurring

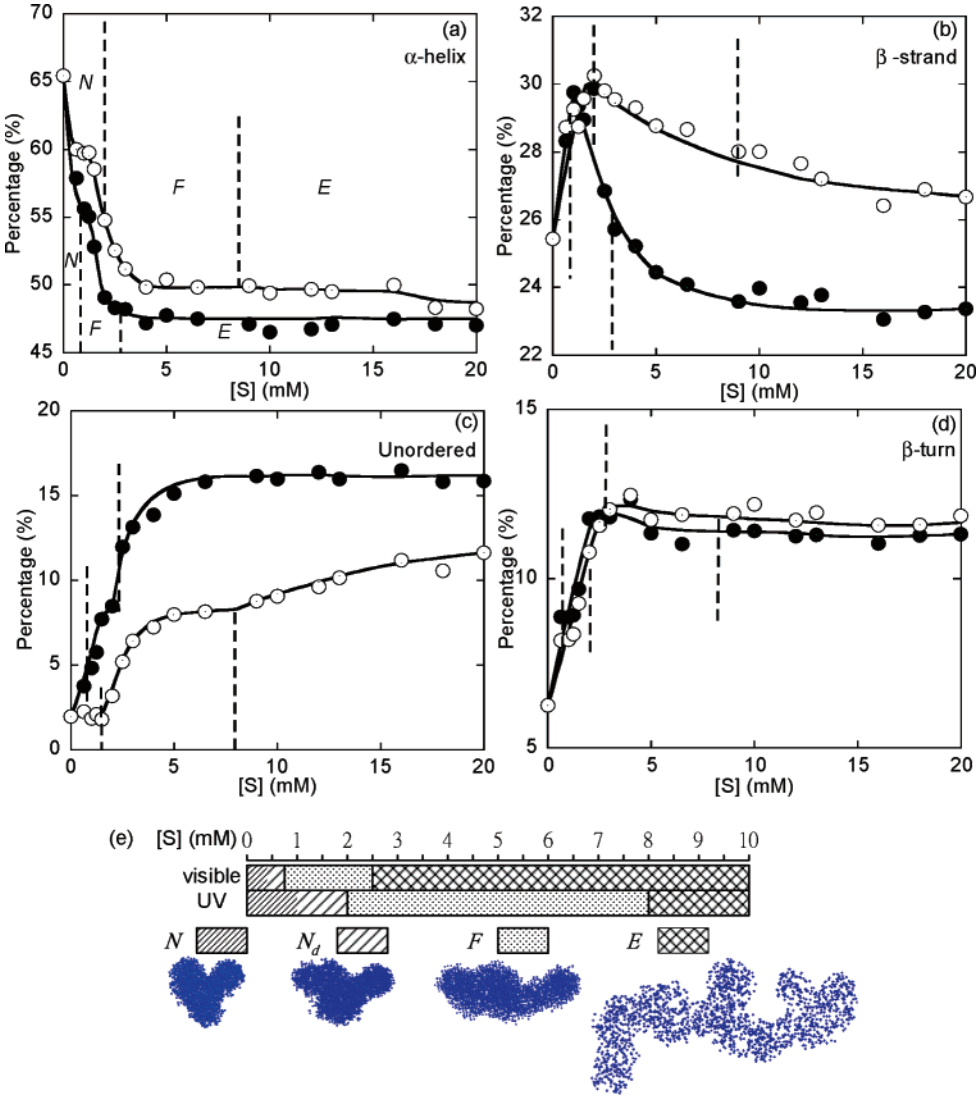

Figure 3. Concentration dependences of the contribution to the secondary structure resulting from (a) α-helix (1653 cm^{-1}), (b) β-strand (1630 cm^{-1}), (c) unordered (1645 cm^{-1}), and (d) β-turn (1677 cm^{-1}) conformations under visible- (○) and UV-light (●) illumination, respectively. The vertical dashed lines in (a)−(d) indicate the tertiary structure boundaries with respect to surfactant concentration obtained from SANS data. The remaining peak from side-chain vibrations was found to increase slightly from 0.9 to 2.5% of the total secondary structure with azoTAB addition. Also shown in (e) are the tertiary structures of BSA under visible- or UV-light illumination from ref 1 as a function of azoTAB surfactant concentration. *N*: native heart-shaped structure; N_d: distorted heart-shaped structure; *F*: partially unfolded; *E*: elongated.

more rapidly under visible light. Combined, these results are consistent with the more-hydrophobic trans form of the surfactant causing a greater degree of unfolding and, hence, more extensive loss of secondary structure in BSA. In the sections that follow, we demonstrate that this apparent complex behavior of the secondary structure elements can in fact be directly related to changes in the protein tertiary structure that were observed with SANS.

Pre-transition. The *in vitro* tertiary structures of BSA obtained through SANS[1] (Figure 3e) revealed that the pure protein exists as a heart-shaped structure in solution (the so-called *N* form), similar to the X-ray crystallographic structure. With the addition of a small amount of azoTAB surfactant (0.55 mM and 1.60 mM under visible and UV light, respectively), BSA was found to adopt a slightly distorted heart-shaped conformation, termed here the N_d form, with the left side of the protein (the C-terminus, or domain III) possibly indicating some degree of swelling. However, from the SANS data alone it was not possible to determine whether this "pre-transition" was indeed a structural rearrangement in BSA or simply a consequence of surfactant accumulating on this part of the protein, since both the protein and bound surfactant molecules scatter neutrons. As shown in Figure 3, however, over the same surfactant concentrations where these subtle differences in BSA tertiary structure were observed, the secondary structure of BSA exhibits dramatic changes. For example, at 0.63 mM azoTAB under visible light (surfactant-to-protein molar ratio, S/P = 4.2) and 1.49 mM azoTAB under UV light (S/P = 10), the helicity of BSA has dropped from 65% to 57.8% and 58.5%, respectively, coinciding with an apparent plateau in the α-helix percentage. Interestingly, this drop of ~7% in helicity is not accompanied by a similar increase in unordered domains; instead, an increase in β-structures is found (from 31.7% for pure BSA to either 37.2% at 0.63 mM azoTAB under visible light or 38.8% at 1.49 mM azoTAB under UV light).

Thus, it appears that the $N \rightarrow N_d$ pre-transition at low surfactant concentrations is a result of an $\alpha \rightarrow \beta$ rearrangement in the protein secondary structure, likely a result of the repulsion of positive charges that develop on the protein upon surfactant binding, which would favor the formation of extended conformations.[24] Similar $\alpha \rightarrow \beta$ transitions have been observed with FT-IR upon the interaction of serum albumin with acid,[24] or

small organic molecules,[32,33,38,39] while the β-sheet percentage of BSA begins to increase at sodium dodecyl sulfate (SDS) concentrations as low as 0.25 mM (S/P = 25).[17] Due to the relatively low surfactant concentrations required to initiate the $N \rightarrow N_d$ conformational change shown in Figure 3, it is likely that this pre-transition is a result of surfactant molecules interacting with high-affinity binding sites on the protein. For comparison, the five binding sites for myristic acid with BSA have been located with X-ray crystallography to be predominantly within hydrophobic pockets of serum albumin (one in subdomain IB, one between IA and IIA, two in IIIA, and one in IIIB).[40] Thus, the FT-IR and SANS results support the idea of the $N \rightarrow N_d$ pre-transition being a result of an $\alpha \rightarrow \beta$ rearrangement in the protein secondary structure, possibly in domain III.

***N* → *F* Transition.** Following the pre-transition, analysis of the SANS data revealed that BSA unfolded to a partially unfolded *F* form at surfactant concentrations of approximately 0.7 mM and 1.9 mM under visible and UV light, respectively. As seen in Figure 3, as this $N \rightarrow$ F transition is crossed the α-helix percentage of BSA undergoes a second decrease of ~10%, now accompanied by a similar increase in unordered structures. At the same time, the percentage of total β-structures remains largely unchanged, with the β-turn proportion increase being offset by the β-strand decrease. Thus, the $N \rightarrow F$ transition appears to be primarily a helical-to-unordered structural transition of the protein. Similar helical-to-unordered transitions have been observed in many proteins with unfolding, and in the case of BSA both thermal[26,41] and chemical (urea or guanidine hydrochloride) denaturation[42] have been shown to disrupt α-helices in favor of unordered structures. Furthermore, ionic surfactants (e.g., SDS and dodecyltrimethylammonium bromide (DTAB)) have also been shown to induce helical-to-unordered transitions in BSA, in some cases accompanied with a slight increase in β-structures.[17]

Interestingly, within the *F*-form region at higher surfactant concentrations, the α-helix content gradually reaches a constant value with no further decrease observed at higher surfactant concentrations. The fact that the remaining helical content is relatively large (~47% under visible light and ~50% under UV light) agrees with the suggestion proposed by Takeda et al. that surfactants (e.g., sodium *n*-alkyl sulfates and *n*-alkyl trimethylammonium bromides) do not disrupt the helical structure in the six large loops in BSA.[17] Similar values of this residual helical content in "unfolded" BSA have been reported with thermal (44% at 65 °C),[41] acidic (~42%),[43] or surfactant (47−53%)[17,44] denaturation. However, judging BSA unfolding solely from the helical content in Figure 3 would result in erroneous estimates of the degree of denaturation, since the most dramatic unfolding (the $F \rightarrow E$ transition discussed below) occurs independently of loss of helical structure. This illustrates the importance of combined secondary and tertiary structure measurements in protein folding studies.

***F* → *E* Transition.** Increasing the azoTAB concentration into the region where BSA adopts the aforementioned elongated *E* form, while not demonstrating any significant changes in the helical structure (indeed, the "kinks" observed in the *E* form from SANS are consistent with these unfolded α-helical segments), does result in an increase of unordered structures with a decrease in β-structures. Similar β-to-unordered transitions induced by surfactant has been observed in immunoglobulin G (IgG) which contains a large amount of β-structure.[45] In the presence of SDS/Tween 20 at 20 °C, a significant amount of IgG β-sheets are transformed to unordered structures due to the destabilizing effect of the hydrophobic surfactant tails penetrating the hydrophobic domains of the protein and weakening the intramolecular hydrophobic interactions within the protein.

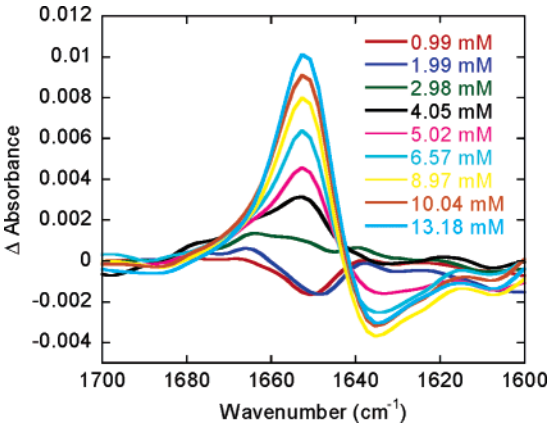

Figure 4. Difference spectra of BSA defined as ΔA = spectra collected under UV light − spectra collected under visible light at a constant surfactant concentration in the amide I region.

Overall, the secondary structure profiles indicate that with visible-light illumination (azoTAB in the relatively hydrophobic trans state) BSA is more unfolded, exhibits less α-helical and β-structures, and has more unordered domains compared to UV-light illumination (hydrophilic cis form). This observation is consistent with studies of BSA unfolding induced by a variety of sodium *n*-alkyl sulfate and *n*-alkyl trimethylammonium bromides surfactants, where it was shown that increasing the length of the alkyl tail (resulting in a more hydrophobic surfactant) lowered the surfactant concentration required to unfold the protein.[19] In addition, there are some more subtle differences between the effects of the trans and cis isomers of azoTAB on BSA unfolding that cannot be explained by simple differences in hydrophobicity. Under visible light, the final values of the α-helical, β-sheet, and random structures at high azoTAB concentrations all differ from the asymptotic values under UV light, implying a fundamental difference in the mechanisms of interaction of the planar trans and bent cis isomers of azoTAB with the protein. Indeed, it would be expected that the trans conformation of azoTAB would present less steric hindrance for the hydrophobic interaction of the benzene rings of the surfactant with the protein. Thus, some moieties of the protein could be inaccessible to the relatively bulky cis form of azoTAB, thereby resulting in a slightly smaller degree of BSA unfolding.

Difference Spectroscopy. To compare the effects of visible- and UV-light illumination on the secondary structure of BSA in azoTAB solutions, difference spectra were calculated by subtracting the protein spectrum obtained under visible light from the spectrum under UV light at a given surfactant concentration, as shown in Figure 4. Positive peaks in the difference spectra then correspond to an increase in absorbance upon illumination with UV light, while negative values indicate that the absorbance is greater under visible light. At low surfactant concentrations (<1.99 mM) a broad negative peak at ~1650 cm^{-1} is observed, which could be resolved through Fourier self-deconvolution (data not shown) into a positive peak at 1656 cm^{-1}, a negative peak at 1651 cm^{-1}, and a broad negative peak at 1645 cm^{-1}. The negative peak at 1645 cm^{-1} indicates that unordered structures appear at the early stages of azoTAB-initiated protein unfolding under visible light (e.g., this negative peak was seen at [azoTAB] as low as 0.99 mM under visible light, see also Figure 3c). The peaks at 1656 and 1651

cm^{-1} are likely due to a shift of the α-helix band to lower wavenumbers caused by a conformational or environmental change upon protein unfolding.[25,46] Specifically, solvent (D_2O) would have a higher accessibility to the protein under visible light (BSA exists as the *N* form under UV light and the *F* form under visible light at 1 mM azoTAB), leading to an increase in hydrogen (deuterium) bonding along the polypeptide backbone, well-known to cause a shift of the α-helix band to lower wavenumbers.[46] The difference spectra at low azoTAB concentration also display an upward-trending peak at ~1640 cm^{-1}, agreeing with the previous observations in Figure 2 that the "hydrated peak" associated with bound water molecules is less prevalent under visible versus UV light. As the surfactant concentration is increased from 2 to 3 mM, the difference spectra in the helical region invert to positive values, indicating that the mismatch between the α-helix peak positions under visible and UV light no longer exists. Note that this is similar to the azoTAB concentration where BSA exists as the *F* conformation under both visible and UV light (2.21 mM azoTAB), thus, the α-helical segments have approximately the same exposure to solvent, independent of the light conditions.

With further increases in the surfactant concentration an increasingly positive α-helix peak develops in the difference spectra, a result of two separate effects. The relatively hydrophobic trans conformation of azoTAB leads to a greater loss of helical structure in Figure 3a than the cis isomer, which would give the observed positive values in the difference spectra in the helical region in Figure 4. In addition, the width of the α-helix band is observed to increase on going from UV- to visible-light illumination, in agreement with the general correlation between an increase in bandwidth accompanying greater protein flexibility,[47] again related to the fact that the protein is less compact under visible light. The combined effects of a decrease in absorbance along with a broadening of the α-helical band as the surfactant concentration is increased lead to increasingly sharper peaks in the difference spectra.

A negative peak in the difference spectra at ~1635 cm^{-1} becomes evident for azoTAB concentrations greater than 4 mM, which could be deconvoluted into a negative peak at 1645 cm^{-1} (unordered structures, not directly visibly from the difference spectra due to overlap with the strong positive peak at 1651 cm^{-1}) and a relatively small upward-trending peak at ~1630 cm^{-1} (β-strands). Taken as a whole, the difference spectra support the trends observed in the quantitative analysis of the protein secondary structure in Figure 3 and confirm the suggestion that the trans azoTAB surfactant induces more protein unfolding and unordered structures than the cis isomer.

Photoreversible Protein Folding Observed with FT-IR. A primary objective of this study was to demonstrate control of protein conformation in a photoreversible manner. While in the previous SANS study it was demonstrated that the tertiary structure of BSA could be recovered with light illumination,[1] it was not possible to detail the precise changes in the local folding state. As shown in Figure 5, photoreversible control of the BSA secondary structure is indeed observed through repeated visible-light ↔ UV-light cycles. Similar cycles were applied at all of the surfactant concentrations utilized in Figure 3 (data not shown) with similar results (i.e., reversibility within the resolution of the FT-IR technique).

While conformational changes in proteins can be induced by the addition of a variety of chemical denaturants or through changes in temperature or pressure, in many of these cases the changes in protein structure are not reversible, primarily due to exposure of the hydrophobic domains of the protein upon unfolding. For example, while the structural changes in BSA with thermal denaturation are reversible below 50 °C, higher temperatures lead to the formation of intermolecular β-sheets and irreversible aggregation of the protein.[26,41,48] Thus, to achieve truly reversible unfolding typically requires that the hydrophobic moieties of the protein be protected in some manner. For this purpose, surfactants have demonstrated great utility in protein folding studies, where binding of the surfactant to hydrophobic groups inherently protects the unfolded protein from aggregation. In fact, a surfactant-based system was used in one of the few successful examples of reversible unfolding of a membrane protein, where exchanging from a "harsh" to a "mild" detergent through dialysis or rapid mixing permitted the refolding of bacteriorhodopsin.[49−52] In the case of azobenzene-based photoresponsive surfactants, exchanging the nature of the surfactant can be achieved with light illumination, providing a simple and fast technique to reversibly control the conformation of proteins.

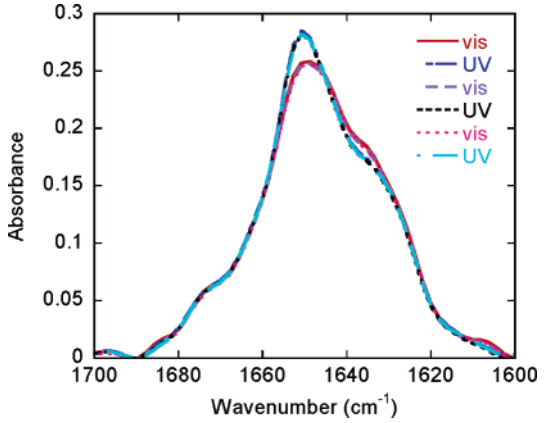

Figure 5. FT-IR spectra of a BSA solution containing 5.02 mM azoTAB under repeated light cycles (visible → UV → visible → UV → visible → UV) in the amide I region.

Conclusion

The ability to control protein conformation at the secondary structure level with light illumination using photoresponsive surfactants has been demonstrated in this study. The visible-light (trans) form of the azobenzene surfactant is more hydrophobic and exhibits more interaction with the protein than the UV-light (cis) form of the surfactant. As a consequence, exposing the surfactant−protein solution to visible light results in a greater degree of protein unfolding, while illuminating with UV light causes surfactant molecules to dissociate from the protein and the protein to refold. The FT-IR spectroscopic data revealed three secondary structure transitions of BSA induced by photoresponsive surfactant and light, related to tertiary structure transitions observed with previous small-angle neutron scattering experiments. At low surfactant concentrations (0.55 mM and 1.60 mM under visible and UV light, respectively), the secondary structure of the protein undergoes an α-helix → β-structure transition, occurring in the same region where the heart-shaped native state of BSA in solution becomes slightly distorted ($N \rightarrow N_d$ transition). Intermediate surfactant concentrations result in an α-helix → unordered structural transition as the tertiary structure of the protein was found to unfold from the native to a partially unfolded conformation (*F* form). At higher surfactant concentrations, a β → unordered transition is observed with the protein adopting a highly elongated shape in solution (*E* form). As a result of these combined secondary and tertiary structure measurements, new insight into the nature of

BSA unfolding was obtained. Finally, the use of photoresponsive surfactants was demonstrated to provide a means to precisely and reversibly unfold/refold proteins with simple light illumination, leading to a new tool in the study of protein folding phenomena.

Acknowledgment. We acknowledge the Charles Lee Powell Foundation and the James H. Zumberge Faculty Research and Innovation Fund for support of this research.

References and Notes

(1) Lee, C. T., Jr.; Smith, K. A.; Hatton, T. A. *Biochemistry* **2005**, *44*, 524.
(2) Hamill, A. C.; Wang, S.-C.; Lee, C. T., Jr. *Biochemistry* **2005**, *44*, 15139.
(3) Reynolds, J. A.; Herbert, S.; Polet, H.; Steinhardt, J. *Biochemistry* **1967**, *6*, 937.
(4) Parker, W.; Song, P. S. *Biophys. J.* **1992**, *61*, 1435.
(5) Ananthapadmanabhan, K. P. *Interact. Surfactants Polym. Proteins* **1993**, 319.
(6) Turro, N. J.; Lei, X.-G.; Ananthapadmanabhan, K. P.; Aronson, M. *Langmuir* **1995**, *11*, 2525.
(7) Hayashita, T.; Kurosawas, T.; Miyata, T.; Tanaka, K.; Igawa, M. *Colloid Polym. Sci.* **1994**, *272*, 1611.
(8) Shin, J. Y.; Abbott, N. L. *Langmuir* **1999**, *15*, 4404.
(9) Eastoe, J.; Dominguez, M. S.; Wyatt, P.; Beeby, A.; Heenan, R. K. *Langmuir* **2002**, *18*, 7837.
(10) Eastoe, J.; Sanchez-Dominguez, M.; Cumber, H.; Burnett, G.; Wyatt, P.; Heenan, R. K. *Langmuir* **2003**, *19*, 6579.
(11) Eastoe, J.; Vesperinas, A. *Soft Matter* **2005**, *1*, 338.
(12) He, X. M.; Carter, D. C. *Nature* **1992**, *358*, 209.
(13) Peters, T., Jr. *All About Albumin: Biochemistry, Genetics, and Medical Applications*; Academic Press: San Diego, CA, 1995.
(14) Carter, D. C. *Adv. Protein Chem.* **1994**, *45*, 153.
(15) Brown, J. R. Serum albumin: amino acid sequence. In *Albumin Structure, Function, and Uses*; Rosenoer, V. M., Oratz, M., Rothschild, M. A., Eds.; Pergamon: Oxford, England, 1977; p 27.
(16) Khan, M. Y. *Biochem. J.* **1986**, *236*, 307.
(17) Takeda, K.; Shigeta, M.; Aoki, K. *J. Colloid Interface Sci.* **1987**, *117*, 120.
(18) Takeda, K.; Moriyama, Y. *Curr. Top. Colloid Interface Sci.* **1997**, *1*, 109.
(19) Takeda, K.; Moriyama, Y.; Hachiya, K. Interaction of Protein with Ionic Surfactants: Part 1. Binding of surfactant to protein and protein fragments, and conformational changes induced by binding. In *Encyclopedia of Surface and Colloid Science*; Hubbard, A., Somasundaran, P., Eds.; Marcel Dekker: New York, 2002; p 2558.
(20) Shang, T.; Smith, K. A.; Hatton, T. A. *Langmuir* **2003**, *19*, 10764.
(21) Le Ny, A.-L.; Lee, C. T., Jr. *J. Am. Chem. Soc.* **2006**, *128*, 6400.
(22) Byler, D. M.; Susi, H. *Biopolymers* **1986**, *25*, 469.
(23) Susi, H.; Byler, D. M. *Methods Enzymol.* **1986**, *130*, 290.
(24) Bramanti, E.; Benedetti, E. *Biopolymers* **1996**, *38*, 639.
(25) Haris, P. I.; Chapman, D. *Biopolymers* **1995**, *37*, 251.
(26) Murayama, K.; Tomida, M. *Biochemistry* **2004**, *43*, 11526.
(27) Fabian, H.; Schultz, C.; Naumann, D.; Landt, O.; Hahn, U.; Saenger, W. *J. Mol. Biol.* **1993**, *232*, 967.
(28) Boulkanz, L.; Balcar, N.; Baron, M.-H. *Appl. Spectrosc.* **1995**, *49*, 1737.
(29) Boulkanz, L.; Vidal-Madjar, C.; Balcar, N.; Baron, M.-H. *J. Colloid Interface Sci.* **1997**, *188*, 58.
(30) Di Nola, A.; Gavuzzo, E.; Mazza, F.; Pochetti, G.; Roccatano, D. *J. Phys. Chem.* **1995**, *99*, 9625.
(31) Kang, J.; Liu, Y.; Xie, M.-X.; Li, S.; Jiang, M.; Wang, Y.-D. *Biochim. Biophys. Acta* **2004**, *1674*, 205.
(32) Purcell, M.; Neault, J. F.; Tajmir-Riahi, H. A. *Biochim. Biophys. Acta* **2000**, *1478*, 61.
(33) Xie, M.-X.; Xu, X.-Y.; Wang, Y.-D. *Biochim. Biophys. Acta, Gen. Subjects* **2005**, *1724*, 215.
(34) Chen, M. C.; Lord, R. C. *J. Am. Chem. Soc.* **1976**, *98*, 990.
(35) Reed, R. G.; Feldhoff, R. C.; Clute, O. L.; Peters, T., Jr. *Biochemistry* **1975**, *14*, 4578.
(36) Pearson, W. R. *Methods Enzymol.* **1990**, *183*, 63.
(37) He, X. M.; Carter, D. C. *Nature (London)* **1992**, *358*, 209.
(38) Neault, J. F.; Tajmir-Riahi, H. A. *Biochim. Biophys. Acta* **1998**, *1384*, 153.
(39) Purcell, M.; Neault, J. F.; Malonga, H.; Arakawa, H.; Carpentier, R.; Tajmir-Riahi, H. A. *Biochim. Biophys. Acta* **2001**, *1548*, 129.
(40) Curry, S.; Mandelkow, H.; Brick, P.; Franks, N. *Nat. Struct.Biol.* **1998**, *5*, 827.
(41) Moriyama, Y.; Kawasaka, Y.; Takeda, K. *J. Colloid Interface Sci.* **2003**, *257*, 41.
(42) Takeda, K.; Sasa, K.; Kawamoto, K.; Wada, A.; Aoki, K. *J. Colloid Interface Sci.* **1988**, *124*, 284.
(43) Muzammil, S.; Kumar, Y.; Tayyab, S. *Eur. J. Biochem./FEBS* **1999**, *266*, 26.
(44) Takeda, K.; Harada, K.; Yamaguchi, K.; Moriyama, Y. *J. Colloid Interface Sci.* **1994**, *164*, 382.
(45) Vermeer, A. W. P.; Norde, W. *Colloids Surf., A: Physicochem. Eng. Aspects* **2000**, *161*, 139.
(46) Jackson, M.; Haris, P. I.; Chapman, D. *Biochemistry* **1991**, *30*, 9681.
(47) Barth, A.; Zscherp, C. *Q. Rev. Biophys.* **2002**, *35*, 369.
(48) Lin, V. J. C.; Koenig, J. L. *Biopolymers* **1976**, *15*, 203.
(49) Marti, T. *J. Biol. Chem.* **1998**, *273*, 9312.
(50) Huang, K. S.; Bayley, H.; Liao, M. J.; London, E.; Khorana, H. G. *J. Biol. Chem.* **1981**, *256*, 3802.
(51) London, E.; Khorana, H. G. *J. Biol. Chem.* **1982**, *257*, 7003.
(52) Chen, G. Q.; Gouaux, E. *Biochemistry* **1999**, *38*, 15380.